Photoresponsive Nanogels Synthesized Using Spiropyrane-Modified Pullulan as Potential Drug Carriers

Bin Wang, Kefu Chen, Ren-dang Yang, Fei Yang, Jin Liu

State Key Laboratory of Pulp and Paper Engineering, South China University of Technology, Guangdong Public Laboratory of Paper Technology and Equipment, Guangzhou 510641, China
Correspondence to: F. Yang (E-mail: yangfei@scut.edu.cn)

ABSTRACT: Reversible light-responsive nanogels were constructed from an amphiphilic spiropyrane-modified pullulan (SpP). The polymer was synthesized by modifying a biodegradable pullulan with carboxyl-containing spiropyrane (Sp) molecules. The SpP structure was confirmed by the appearance of a carbonyl signal in the FT-IR and ^{1}H NMR spectra. The nanogels can be controlled by photostimulation, which results in the reversible structural transformation of the hydrophobic Sp to the hydrophilic merocyanine. The physical properties of the nanogels were confirmed to change dramatically after being irradiated with different wavelengths of light. Drug delivery tests showed that the model drug pyrene was completely captured by the nanogels and then released from the SpP nanogels in a light-dependent manner. This study provides an alternative approach to constructing light-responsive nanocarriers with excellent biocompatibility for drug uptake and release. © 2013 Wiley Periodicals, Inc. J. Appl. Polym. Sci. **2014**, *131*, 40288.

INTRODUCTION

Nanogels have been widely used in fields such as fabrication of sensing devices,[1,2] gene diagnostics,[3] bioengineering,[4,5] and other areas.[6,7] Nanogels have also been used in drug delivery. In numerous instances, nanostructured carriers show more efficient drug-release effects than macrosized systems. Given their large surface areas, diseased cells can be targeted by nanodrug delivery systems via attachment to the drug surface. Nanogels and other nanosized drug-delivery systems can be physically embedded in cells and subsequently released by diffusion.[8–10]

Various external stimulus-sensitive nanogels have been developed and have been increasingly used because of their superior properties. Numerous physical and chemical stimuli, including temperature, light, pressure, sound, pH, and ions,[11–14] have been applied to polymers to prepare stimulus-responsive hydrogels (nanogels) via molecular design. Light is a particularly attractive option because its intensity and wavelength can be readily, remotely, and accurately controlled.[15–17] Light-responsive hydrogels are stimulated at the target site through selective light irradiation, and drugs are released to treat viral infections. Light-responsive hydrogels can accurately deliver doses specific to individual patients through wavelength adjustments.[18–24]

Another important aspect of delivery is material selection. As a renewable resource, starch is low cost and exhibits high biocompatibility and biodegradability. Aside from its applications in the food industry, starch is also used as an excipient, stabilizer, and slow-release drug system. Starch-based materials have high biocompatibility compared with other drug-release systems. Starch primarily contains two different types of glucose chains: the unbranched amylose, which exhibits an α(1–4) linkage, and the branched pullulan, which has an α(1–6) linkage. Pullulan is water-soluble, edible polysaccharide produced from starch by the fungus *Aureobasidium pullulans*.

Extensive studies have been conducted on the modification of starch derivatives for different applications.[25–27] Na and Bae[28] have synthesized pH-responsive hydrogels of pullulan acetate and sulfonamide. The pH-responsive nanoparticles can be used for targeted anticancer drug delivery because of the aggregation of these particles at different pH. Chen et al.[29] have synthesized polyphosphate with carboxyl-containing spiropyrane (Sp) molecules and successfully encapsulated a model drug into the micelles. The smart nanocarriers exhibit high performance in controlling the release and re-encapsulation of hydrophobic drugs. Light-responsive block copolymer[30] micelles containing Sp self-assemble into reversible light-responsive micelles in aqueous solutions. The issue of the excitation wavelength for biomedical applications was also addressed in this work. However, the use of starch as a raw material for the light-responsive drug-delivery systems has not been evaluated.

Sps are a group of colorless, light-switchable, "spiroform" molecules that absorb only ultraviolet (UV) light. When Sp undergoes isomerization, it changes into merocyanine (Mer) under UV or thermal stimulation. When the Mer molecule is exposed to visible light, it reverts into Sp (Scheme 1). This reversible photochemical process is possibly biocompatible because no free radicals are generated.

In this study, Sp-modified pullulan (SpP) was designed and synthesized using carboxyl-containing Sp (Sp-COOH) and pullulan (Scheme 1). The morphologies and crystallinities of both native and modified pullulan were analyzed by scanning electron microscopy (SEM) and X-ray diffraction (XRD). The polymer can self-assemble into reversible, light-responsive nanogels in aqueous solutions. To our knowledge, the use of edible materials for constructing reversible light-responsive nanogels using a simple method has never been previously reported. These nanogels were analyzed by multiangle laser light scattering (MALLS), dynamic light scatting (DLS), Fourier transform infrared (FT-IR) spectroscopy, proton nuclear magnetic resonance (¹H NMR) spectroscopy, and atomic force microscopy (AFM). Drug uptake and release were determined using UV spectrophotometry. The distribution of absorbed fluorescently labeled drug throughout the nanogel particles was determined using confocal laser scanning microscopy (CLSM). The drug uptake and release properties were investigated by using pyrene as a model drug. Finally, the nanogel-encapsulated drugs and their release were analyzed.

EXPERIMENTAL

Materials

Pullulan maize starch was purchased from TCI (Tokyo Kasei Kogyo, Japan) and dried at 50°C for 24 h prior to use. 3-Bromopropanoic acid, 5-nitrosalicylaldehyde, pyrene (98%), and 2,3,3-trimethylindolenine were obtained from Acros (Beijing InnoChem Science & Technology, China). All other chemicals were reagent-grade, purchased from commercial sources, and used without further purification. Water (18.2 MΩ) was purified with a Millipore Milli-Q system. UV and visible-light irradiation were generated by an 8 W UV lamp (354 nm) and 8 W white-light lamp (620 nm) with an intensity of 2 mW/cm², respectively.

Synthesis of 2-(2,3,3-Trimethylindolin-1-yl) Propanoic Acid (C-TMI-Br)

The quaternary salt C-TMI-Br was synthesized using a previously described method.[31] A solution of 2,3,3-trimethylindolenine (4.42 g, 272 mmol) and 3-bromopropanoic acid (4.27 g, 272 mmol) in 20 mL of chloroform was refluxed for 20 h. Water (50-mL) was then added to the mixture. The product (6.52 g, 75% yield) was obtained through extraction and washing with chloroform followed by distillation at reduced pressure.

Synthesis of 3-(3′,3′-Dimethyl-6-nitrospiro[chromene-2,2′-indolin]-1′-yl) Propanoic Acid (Sp-COOH)

Approximately 1.68 g (10.0 mmol) of 5-nitrosalicylaldehyde in 32 mL of ethanol was added dropwise to 3.13 g (10.0 mmol) of C-TMI-Br in 80 mL of ethanol.[32] The mixture was then refluxed for 10 h. The purple mixture was placed in a reasonably cool
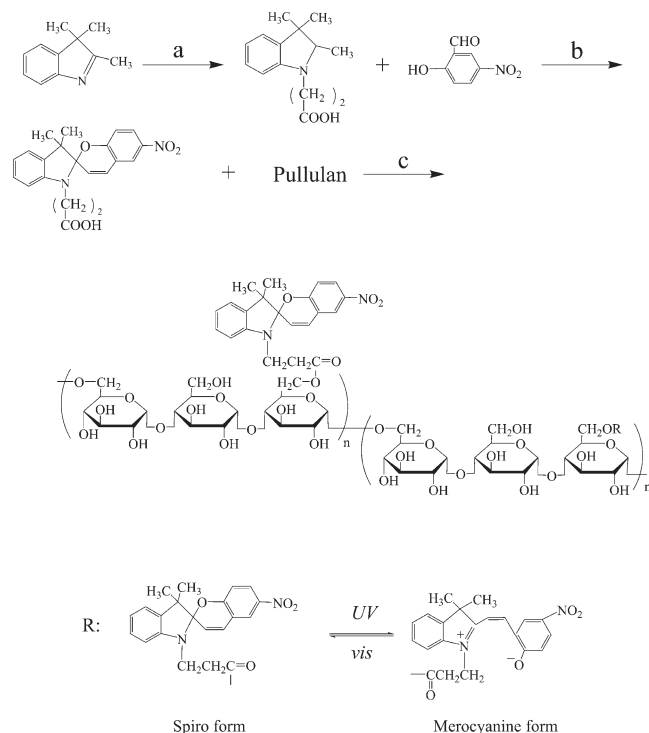
Scheme 1. Synthesis of SpP. (a) 3-Bromopropanoic acid, chloroform, 60°C, 20 h. (b) 5-Nitrosalicylaldehyde, ethanol, 70°C, 10 h. (c) DCC, DMAP, DMSO, 25°C, 40 h.

place for at least 6 h and then filtered. The filter cake was washed with methanol to obtain an orange solid (2.50 g, 52% yield).

SpP Synthesis

SpP was synthesized in a 100 mL three-necked round flask using a Schenk line. Exactly 572 mg (1.52 mmol) of Sp-COOH was dissolved in 10 mL of dimethyl sulfoxide (DMSO), and the solution was kept under gaseous Ar. Afterward, dicyclohexyl carbodiimide (DCC; 310 mg, 1.52 mmol) and 4-(N,N-dimethylamino)pyridine (DMAP; 30 mg, 0.25 mmol) were rapidly added into the flask. A Pullulan-DMSO solution (1.0 g of pullulan dissolved in 30 mL of DMSO) was injected into the flask, and the reaction solution was heated to 40°C for 40 h. Finally, the product was purified by adding 50 mL of acetone to the reaction mixture and centrifuging for 5 min at 4000 r/min. The precipitate was washed with acetone and dried in a vacuum oven. After drying, the target-modified pullulan was further dissolved in DMSO in a loaded dialysis bag (molecular weight cutoff, 3,500) against deionized water for 7 days to remove residual monomers and initiators. Finally, the product was obtained by freeze-drying (79% yield) and was characterized by IR (Nexus 470, Thermo Nicolet) and ¹H NMR (400 MHz, AVANCE AV 400, Bruker, Switzerland) spectroscopy. The results for the samples dissolved in DMSO [d_6/D$_2$O = 10/1 (v/v)] are as follows: δ 4.75 [s, 33H (per 100 glucose units), pullulan C¹H (1–6)], 5.05 [d, 66H (per 100 glucose units), pullulan C¹H (1–4)], and 6.00–7.20 (m, 6H, aromatic H of indoline).

Characterization of Sp Acid Pullulan Esters

The FT-IR spectra for native pullulan and Sp acid pullulan esters were recorded with a Nexus 470 spectrophotometer

(Thermo Nicolet). The samples were mixed and ground with KBr for IR measurements within the frequency range of 400–4000 cm^{-1}. ^{1}H NMR spectra were recorded with a Bruker 400 MHz (AVANCE AV 400, Switzerland). The sample was dissolved in deuterated DMSO (DMSO-d_6) at 30°C. The SEM images of the samples were obtained using a Hitachi S-2500 SEM (Hitachi, Tokyo, Japan) at an acceleration voltage of 25 kV. The samples were mounted on an aluminum stub using a double sticky tape. The samples were then coated with gold under vacuum prior to analysis. The XRD patterns were recorded with a D8 ADVANCE diffractometer (Bruker, German) with Cu Kα filtered radiation ($\lambda = 0.154$ nm) and operating at a voltage of 40 kV and a current density of 40 mA. The scanning range (2θ) was from 5° to 45° at a scan rate of 2°/s and a step width of 0.02°.

Preparation of SpP Nanogels

SpP nanogels were prepared through dialysis. Exactly 30 mg of SpP was dissolved in 2 mL of DMSO at room temperature. Afterward, 2 mL of deionized water was added dropwise into the solution. After stirring for 3 h, the solution was dialyzed against deionized water in a dialysis bag (molecular weight cutoff, 3500) for 3 days to remove the DMSO. The nanogels were then transferred into a 10 mL volumetric flask, which was filled to the mark with purified water.

DLS Measurements

DLS measurements were conducted using a Zetasizer Nano ZS instrument (Malvern Instruments, Malvern, UK) equipped with a Peltier temperature control unit. The analyses were performed at a wavelength of 632.8 nm and a detection angle of 90°. The hydrodynamic diameters of the SpP self-aggregates were calculated by the Laplace inversion program CONTIN. Each SpP nanogel sample was prepared by exposure to visible light for 120 min or to UV light for 30 min.

Surface-Tension Measurements

Surface tension was measured using the contact angle measurement (Dataphysics OCA40 Micro, Germany) with SCA22 control and analysis software. Each SpP nanogel sample (1 mg/mL) was prepared by exposure to visible light for 120 min or to UV light for 30 min.

MALLS Measurements

Gel permeation chromatography (GPC) was performed using a chromatography system with a refractive index detector (Optilab rEx, Wyatt) connected to a MALLS detector (DAWN HELEOS-II Wyatt Technology, Santa Barbara, CA). A 10 mM aqueous NaCl solution was used as a mobile phase at 0.8 mg/mL. The molecular weight (M_w) and root-mean-square of gyration (R_g) of the SpP2 sample were used in the column GPC-MALLS measurements. These data were determined by the equipped ASTRA software based on Zimm's equation. The flow rate of the nanogel solutions (2.0 mg/mL) was 0.50 mL/min at 35°C. The refractive index increment (dn/dc) was 0.151 mL/g, as determined by an Optilab DSP (Wyatt Technology, Santa Barbara, CA). The nanogel solutions were passed through 0.22 μm filters prior to application to the column. Each SpP nanogel sample was prepared by exposure to visible light for 120 min or to UV light for 30 min.

Atomic Force Microscopy

An aqueous SpP solution (1 mg/mL) was dropped onto a transparent mica substrate, and the solution was evaporated in an IR oven. The crystalline morphologies of the nanogels were examined under an AFM (Nanoscope IIIa MultiMode SPM, Japan) at 20°C using a Si probe (RTESP, Seiko) with a spring constant of 15 N/m.

Drug Uptake Capacity

Specific amounts of pyrene were dissolved in different volumes of DMSO. An intensity–concentration standard curve was established using UV spectrophotometry (Agilent 8453). Exactly 10.0 mg of the polymer and 2.0 mg of pyrene were dissolved in 2.0 mL of DMSO under stirring. The mixed solution was dialyzed for 24 h against deionized water using a dialysis bag (MWCO = 3500); water was changed every 4 h. The resultant SpP concentration in the solution was adjusted to 1 mg/mL. The amount of loaded drug in the micelles (W_p) was calculated from the UV–vis absorbance at 303 nm relative to the calibration curve. The loading efficiency (E_L) and drug content (C_D) were calculated as follows[33]:

$$E_L = W_p / W_t \times 100\%$$

$$C_D = W_p / W_m \times 100\%$$

where W_p, W_t, and W_m are the mass of pyrene in the nanogels, total mass of pyrene used, and nanogel mass, respectively. The hydrodynamic diameter (D_h) distribution of the pyrene-loaded nanogels was determined by DLS.

Drug Release

The release behavior of the loaded pyrene from the nanogels was determined as follows: 5 mL of an aqueous solution of drug-loaded micelles was dialyzed (molecular weight cutoff, 14,000) in a beaker with 200 mL 1 × PBS (PBS: 10 mM phosphate-buffered saline, 137 mM NaCl, 2.7 mM KCl, pH 7.4) at 37°C. The nanogels were exposed to different types of light (620 nm visible light for the entire experiment, 354 nm UV light for 5 min, or in the dark for the entire experiment). Pyrene can diffuse from the solution in the dialysis bag to the buffer solution. Approximately 30 μL of the dialysate was collected at certain time intervals and then diluted to 5 mL with DMSO. The pyrene concentrations at different time intervals were determined by comparing the absorption intensity at 303 nm relative to the calibration curve as described in Drug Uptake Capacity.

RESULTS AND DISCUSSION

An esterification reaction was performed to prepare Sp acid pullulan esters under mild conditions. The reaction of pullulan with Sp-COOH generated products with different degrees of carbonyl-group substitutions (DS) in the pullulan main chain.

^{13}C NMR Spectra for Sp-COOH

Sp-COOH was prepared via aldol condensation using Fischer indole synthesis and salicylaldehyde. A carboxylic acid group was first introduced into the nitrogen atom of indole via alkylation. The condensation reaction of Sp-COOH with 5-nitrosalicylaldehyde was then performed to yield Sp-COOH products (Scheme 1). Figure 2 shows the ^{13}C NMR spectra for

Table I. Chemical Characteristics of the SpS Nanogels

abb.	Sp-COOH: Pullulan	DS[a] (100 glucose units)	M_n[a] ($\times 10^5$)	Yield (%)
SpS1[b]	1:8	0.92	1.12	78.5
SpS2[b]	1:4	1.87	1.15	42.8
SpS5[b]	1:2	4.52	1.23	30.4

[a] Degree of substitution (DS) was determined by ^{1}H NMR: $H_p/(DS*H_I)$= S_p/S_I, DS (SpS2)= $(H_p*S_I)/(H_I*S_p)$=66×0.17/(6×1)= 1.87, where H_p, H_I, S_p, and S_p are the H (1-4) of the pullulan glucose units, aromatic H of indoline, the area of H (1-4) of the pullulan glucose, and the area of aromatic H of indoline respectively.
[b] Polymerized at 40°C for 40 h. DCC and DMAP were added as catalytic agent.

C-TMI-Br [Figure 2(a)] and Sp-COOH [Figure 2(b)]. The carboxyl C of C-TMI-Br is indicated by the peak at 174 ppm [Figure 2(a)]. Moreover, the ^{13}C NMR characteristic peaks of C-TMI-Br are found at 28, 31, 48, and 72 ppm. The ^{13}C NMR spectra for Sp-COOH exhibit new peaks [Figure 2(b)] within the 105–160 ppm range. Comparison with the characteristic peaks of C-TMI-Br indicates that the new peaks correspond to benzene-ring C. These results confirm the successful synthesis of Sp-COOH via aldol condensation.

^{1}H NMR Spectra for SpP

This synthesis strategy was performed by reacting Sp-COOH with pullulan (Scheme 1). A series of SpP polymers (Table I) were prepared by varying the molar ratios of Sp-COOH and pullulan. The DS and relative molar amounts of the SpP samples were obtained from the ^{1}H NMR signals at 6.0–7.2 ppm, which are attributed to aromatic H of indoline in the Sp-COOH units, and from the signals at 5.18–5.31 ppm, which are ascribed to [1]H (1–4) of the pullulan glucose units (Figure 3). The chemical composition of the SpP samples, the number average molecular weight (M_n), and the DS of the Sp-COOH group in pullulan were determined from these signals; the results are listed in Table I.

FT-IR Spectra for Native Pullulan and SpP

Figure 4 shows the FT-IR spectra for native pullulan [Figure 4(a)], SpS1 with 0.92 DS [Figure 4(b)], SpS2 with 1.87 DS [Figure 4(c)], and SpS5 with 4.52 DS [Figure 4(d)]. The band at 3377 cm^{-1} is assigned to OH stretching of pullulan, and the strong signal at 2930 cm^{-1} is attributed to CH stretching. In the spectrum for native pullulan, COH and COC stretching in the anhydrous glucose ring are indicated by the bands at 1151, 1081, and 1020 cm^{-1}.

Figure 4(a–d) show the combined characteristic absorption peaks of pullulan and SpP. The presence of the CO band confirms the formation of SPCOO-modified pullulan. Compared with that of native pullulan, the spectrum for the modified pullulan shows an additional band at 1740 cm^{-1} [Figure 4(b–d)]. The band at 1740 cm^{-1} is due to the carbonyl group CO and is indicative of ester formation. As the DS increases, the area of the carbonyl peak at 1740 cm^{-1} gradually increases. Similar carbonyl vibration peaks were also observed in previous studies.[34,35]

SEM Analysis of Native Pullulan and SpP

SEM was used to investigate the morphological changes of native pullulan and Sp acid pullulan esters. Figure 5(a,b) show that native maize starch is round or exhibits an oval granular shape. Compared with the unmodified pullulan, the Sp acid pullulan esters present a completely different morphology. Figure 5(c–h) show that the pullulan granules are completely distorted. The change in the granular structure can be attributed to esterification. The morphology was severely distorted because of the destruction of the crystalline structure of the starch granules when the molar ratio of Sp-COOH to pullulan was increased.

XRD Analysis of Native Pullulan and SpP

XRD analysis was performed to determine the changes in the crystallinity of pullulan after modification (Figure 6). The XRD pattern for native pullulan [Figure 6(a)] clearly shows strong reflections (2θ) at ~15°, 17°, 18°, and 23°. These occurrence of these signals indicate that native starch exhibits a typical A-type X-ray pattern.[36] However, the characteristic peaks become progressively weaker after modification; however, the peaks observed at ~2θ = 18° are characteristic of V-type starch.[37] These results indicate that the hydrogen bonds were disrupted by esterification. The crystallinity pattern of the Sp acid pullulan esters was converted into a V type, which is consistent with the findings of Lu et al.[38]

Properties of SpP2 Nanogels in Water

The solution properties and photochromic behaviors of SpP in aqueous solutions were investigated by MALLS, DLS, and UV–vis spectroscopy. SpP solutions (1–3 mg/mL) were prepared from a mother solution (3 mg/mL) at 50°C for 10 min to approach the stability of the nanogel solution. DLS results show that the D_h of SpP was 78.96 nm at 1.0 mg/mL and 179.7 nm at 3.0 mg/mL. Meanwhile, MALLS results indicate that the M_w of the nanogels was $(20.2 \pm 4) \times 10^5$. The M_w of the aggregates indicate that these nanoparticles consist of ~20 macromolecules, given that the M_w of one SpP molecule is 1.15×10^5 g/mol.
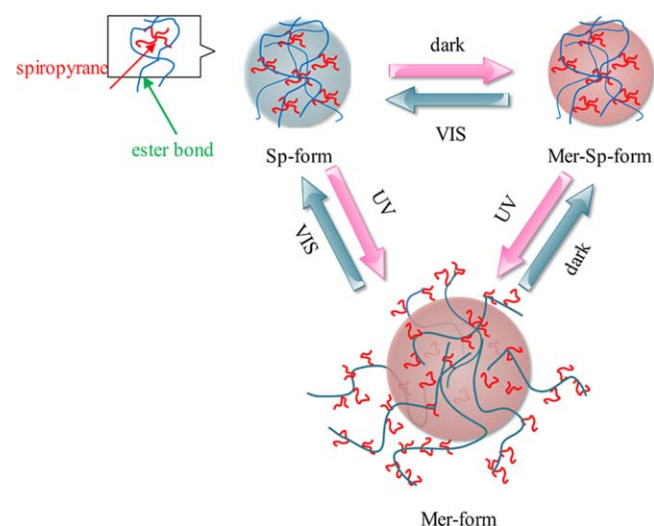

Figure 1. Schematic illustration of SpS nanogel at UV and vis. [Color figure can be viewed in the online issue, which is available at wileyonlinelibrary.com.]
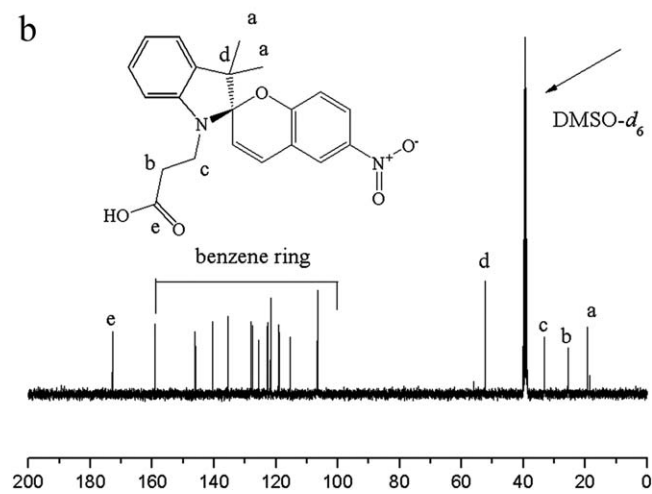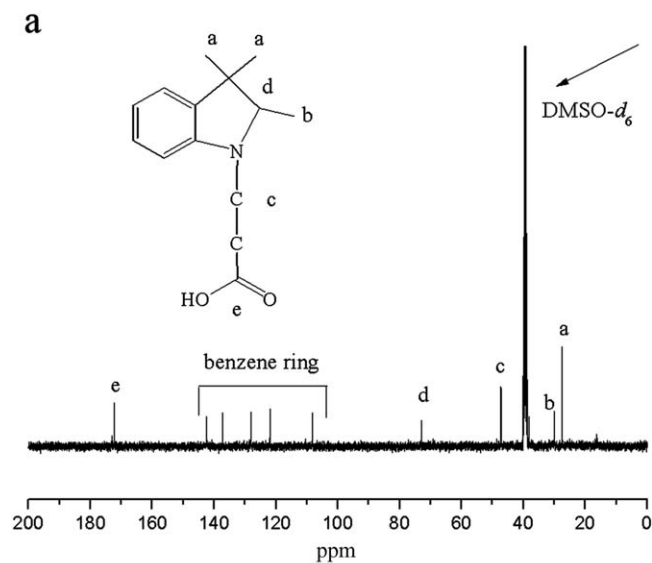
Figure 3. ^{1}H NMR spectra of SpP2.

size (D_h, 77.27 nm) and M_w [(16.2 ± 4) × 10^5 g/mol] of the nanogels both showed negligible changes. Afterward, nanogels were placed in the dark, and the colored Mer (515 nm) gradually reappeared within 3 h (Figure 7). However, UV light was irradiated onto the dark adaptation of the sample, the sample solution turned red. The maximum absorption wavelengths shifted to 535 nm (Figure 7), and the size and M_w both increased during UV irradiation [5 min, 114.1 nm (33.3 ± 2) × 10^5 g/mol; 30 min, 134.4 nm, (74 ± 4) × 10^5 g/mol].

D_h and M_w significantly increased under UV radiation. This increase can be explained by particle aggregation in the nanogel solutions. Moreover, the effects of UV on D_h and M_w were reversible, and the nanogels were recovered after exposing visible light (Figure 1). The red color disappeared during the cycled procedure only after 2 h. The D_h of the micelles also caused

Figure 2. ^{13}C NMR spectra of C-TMI-Br and Sp-COOH: (a) C-TMI-Br; (b) Sp-COOH.

The average density of each nanoparticle ($Ø_h$) was calculated as ∼0.016 mg/mL using the following equation[39,39]:

$$Ø_h = M_w/N_A × (4/3πR_h^3)^{-1}$$

where N_A is Avogadro's number. These results suggest that the nanoparticles act as nanogels that contain ∼0.09 wt % cross-linking points from the Sp groups in the polysaccharide macromolecules.[40]

The nanogels turned red when these samples were placed in the dark for a few minutes. Moreover, UV results show that the wavelength of maximum absorbance for the resulting red solution is 515 nm. When the nanogels were irradiated with visible light (620 nm), the red color gradually disappeared, and no maximum absorption was observed in the 400–600 nm range. These results indicate that the colored open Mer was transformed into the colorless close spiroform (Sp; Figure 7, Scheme 1, bottom portion). After exposure to visible light for a certain period, the
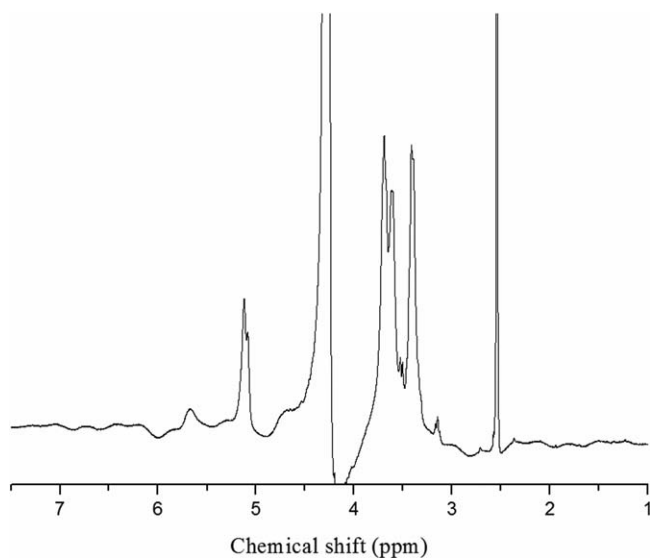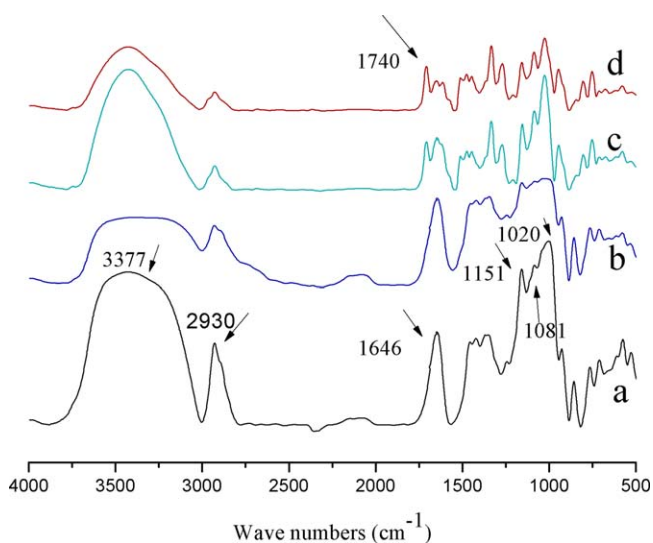

Figure 4. FT-IR spectra: (a) native pullulan; (b) SpS1 (DS 0.92); (c) SpS2 (DS 1.87); (d) SpS 5(DS 4.52). [Color figure can be viewed in the online issue, which is available at wileyonlinelibrary.com.]
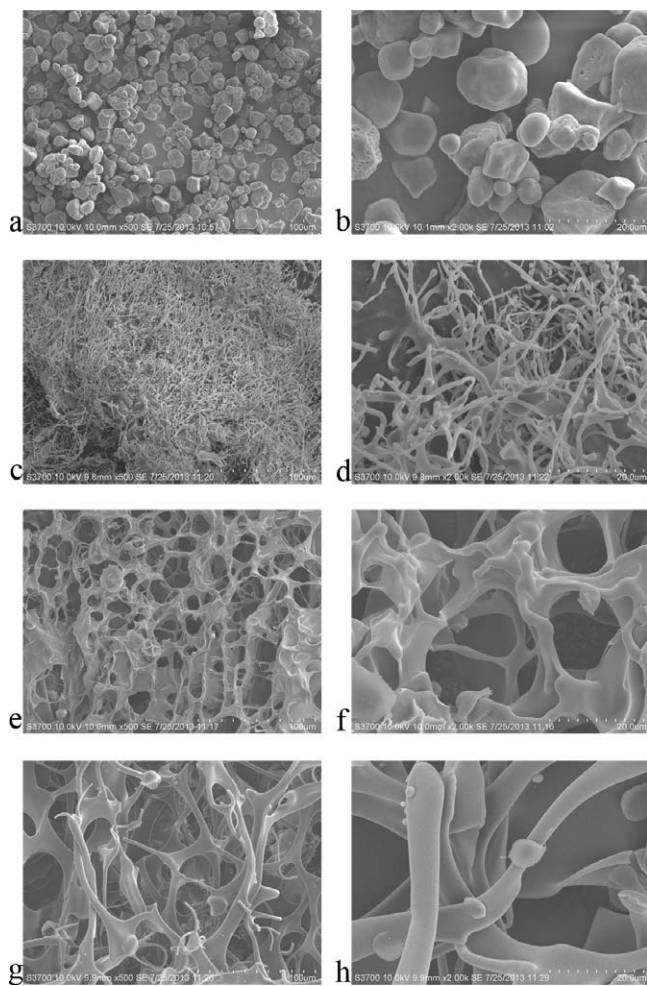
Figure 5. SEM images of starch: (a) native pullulan ×500; (b) native pullulan ×2000; (c) Sp acid pullulan esters ×5000; (d) Sp acid pullulan esters 2000 (DS 0.92); (e) Sp acid pullulan esters ×500; (f) Sp acid pullulan esters ×2000 (DS 1.87); (g) Sp acid pullulan esters ×500; (h) Sp acid pullulan esters ×2000 (DS 4.52).
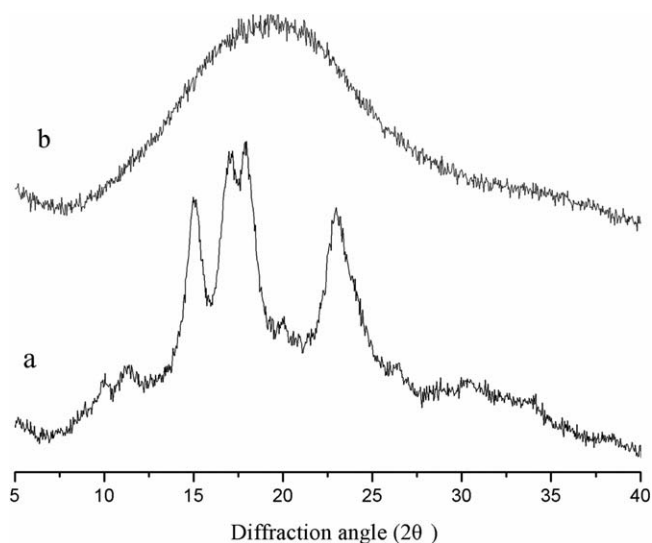

Figure 6. XRD spectra: (a) native pullulan; (b) Sp acid pullulan esters.
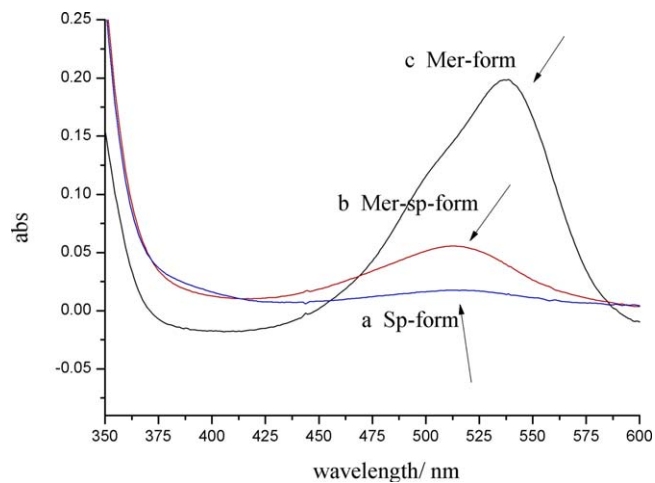

Figure 7. UV–vis spectrum of the photochromism of SpS (0.3 mg/mL) nanogels solution. (a) Sp-form visible light for 2 h, (b) Mer-sp-form under dark, and (c) Mer-form UV light for 15 min. [Color figure can be viewed in the online issue, which is available at wileyonlinelibrary.com.]
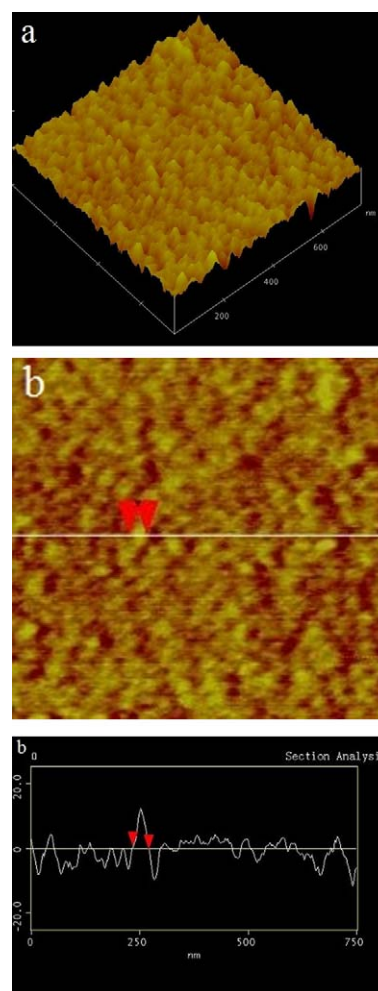

Figure 8. AFM images of SpS2 nanogels, (a), three-dimensional image for nanogels and (b), section analysis for nanogels. [Color figure can be viewed in the online issue, which is available at wileyonlinelibrary.com.]

Table II. The Loading Efficiency and Pyrene Content of SpP Nanogels

m (SpP) : m (drug)	Loading efficiency (E_L; %)	Drug content (C_D; %)
2.5 : 1	7.1	2.8
5 : 1	15.3	3.0
10 : 1	31.8	3.2

slight shrinking until the original size of the Sp form (77.29 nm) was reached.

In the experiments, the wavelength of maximum absorbance shifted to 535 nm after the nanogels were exposed to UV radiation. This result indicates that the structure of the SpP nanogels also changed. The micelles clearly reverted to their previous forms when the nanogels were heated at 50°C for 5 min. According to literature,[41] the open Mer structures tend to form dimers or oligomers. In summary, the synthesized SpP nanogels exist in the following three states: Mer-Sp-form (515 nm), Mer-form (535 nm), and Sp-form (Figure 1).

The surface properties of the nanogels also changed during the photochromic process. The surface tension of the Mer-Sp-form nanogels (1 mol/mL, under dark) was 58.84 mN/m, whereas that of the Sp-form nanogels prepared by visible-light irradiation of the Mer-Sp-form solution for 60 min was 55.28 mN/m. Meanwhile, the surface tension of the Mer-form, which was prepared when the Mer-Sp-form nanogels were exposed to UV light for 1 h, was 53.81 mN/m. Through interfacial tension measurements, we confirmed that the physical properties changed during the light-responsive process, and that the self-assembled process can be controlled by photic stimulation.

A three-dimensional AFM image of SpP2 was obtained by depositing the sample onto a transparent mica substrate (1 mg/mL) [Figure 8(a)]. Individual particles and aggregations of small particles were also detected. Figure 8(b) shows closely packed and regular oviform particles. The geometric size of the cross-section of a single particle was ~70 nm, and the axial ratio was 3 : 1. The results shown in Figure 8 are consistent with the formation of nanogels in solution, as determined by DLS.

Loading and Light-Responsive Release of Pyrene in the SpP Nanogels

In a previous study,[42,43] modified pullulan molecules were used as nanogels for drug loading and release. The results showed that photosensitive nanogels can also be used as drug-delivery vehicles, and their performance can be evaluated. In this study, the loading and controlled releases of drugs (with pyrene as the model drug) by the prepared Sp-bearing pullulan nanogels were investigated. The loading and light-responsive release behaviors of the SpP nanogels and the model drug cargo were analyzed via UV–vis spectrophotometry at 303 nm.

Pyrene was selected because it is a drug with low water solubility as well as sensitive and specific fluorescence. The release behaviors were determined in PBS solutions at pH 7.4. Table II shows the loading efficiencies and pyrene contents in the SpP nanogels at different feeding ratios of SpP to pyrene.

The results indicate that the loading efficiency increased when the feeding ratio of SpP to pyrene increased. The high proportion of SpP relative to pyrene clearly enhanced the particle aggregation, which resulted in the formation of larger amounts of nanogels, which served as carriers of loaded pyrene. However, the change in the pyrene content was not significant when the feeding ratio of SpP to pyrene was increased. This result is mainly due to the structure of the nanogel–pyrene system.[44] As a result, the increase in the feeding ratio of SpP affected the
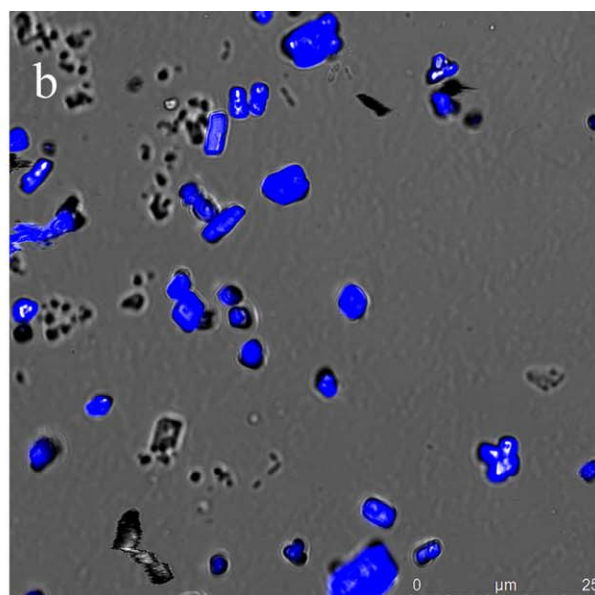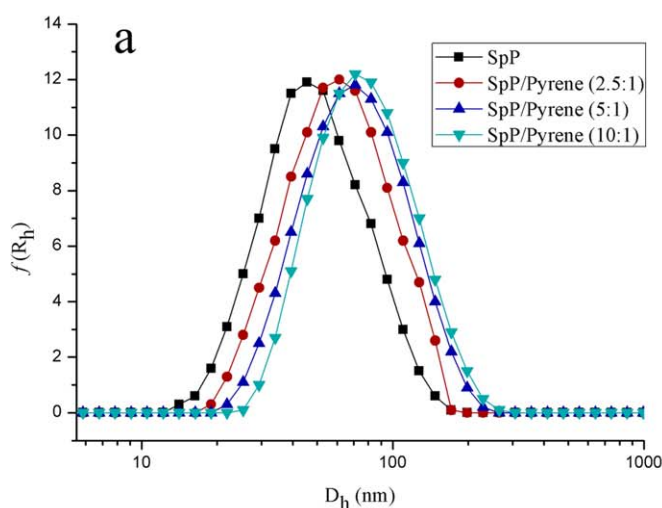

Figure 9. (a) Hydrodynamic diameters distribution of the blank nanogels and pyrene-loading nanogels at SpP to pyrene ration of 2.5 : 1, 5 : 1, and 10 : 1; (b) CLSFM image of Pyrene-loaded nanogels. [Color figure can be viewed in the online issue, which is available at wileyonlinelibrary.com.]
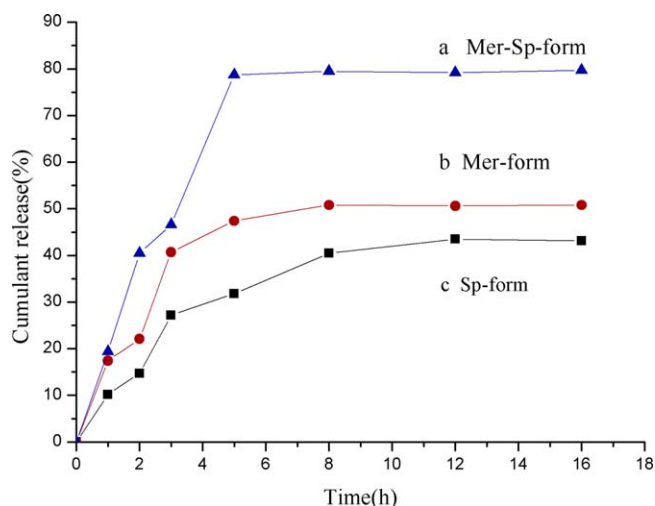
Figure 10. The comparison of pyrene release profile from different nanogels in phosphate buffer pH 7.4. [Color figure can be viewed in the online issue, which is available at wileyonlinelibrary.com.]

loading efficiency and showed weak effects on the loading capacity of the system.

The size distributions of the blank and pyrene-loaded nanogels were determined by DLS [Figure 9(a)]. The average D_h of the blank nanogels is 81 nm. The D_h of the pyrene-loaded nanogel particles were 109, 115, and 131 nm at pyrene contents of 2.8, 3.0, and 4.1%, respectively. These values are slightly higher than those of the blank nanogels. The results confirm the successful drug loading in the nanogels. Figure 9(b) shows the representative laser confocal microscopy image of the pyrene-loaded nanogels. The nanogels are highly dispersed as individual nanoparticles with regular spherical shapes. This uniform dispersion confirms that pyrene was completely internalized into the nanogels.

The release profile of pyrene from the drug-loaded nanogels was obtained in PBS solutions at pH 7.4 over a 16 h period to simulate the blood environment. To evaluate the light-controlled release behavior, the drug-loaded nanogels were exposed to 620 nm of visible light (Sp-form) for the entire experiment, to 354 nm of UV light (Mer-form) for 5 min, and to dark (Mer-Sp-form) for the entire experiment. Figure 10 shows the profiles under different light conditions. Pyrene release largely depended on the state of the drug-loaded nanogels. The initial release rate was highest for the Mer-Sp-form, with the total amount of pyrene release exceeding 80%. By contrast, <50% of pyrene was released by the two other SpP nanogels over 16 h. All of the drug-loaded nanogels exhibited an initial burst release within the first 3 h and then showed sustained release for an extended period. This two-step release profile may be attributed to a concentration gradient.

The release amount and rate decrease in the following order: Mer-Sp-form > Mer-form > Sp-form. This trend shows that the SpP nanogels are stable in the Sp-form because of the "closed ring" structure, which restricts pyrene diffusion or release. Moreover, the low release may be due to the entrapment of pyrene in the hydrophobic core structure of the Sp-form

nanogels. Meanwhile, the relatively high release may be due to the diffusion of absorbed pyrene from the hydrophilic shell of the Mer-form structure. This phenomenon is attributed to the transformation of the hydrophobic SP-form into the hydrophilic Mer-form under UV irradiation. The drug and the drug-loaded nanogels in the surrounding solution might eventually reach equilibrium concentrations, and then the next release of more drug molecules will stop. Thus, the drugs could not be completely released. Finally, electrostatic interaction possibly disappears during the transformation into the Mer-Sp-form.[41] This reduced interaction leads to a considerably faster release of pyrene by this form compared with those by the two other nanogel states after photostimulation. One or more of these factors may explain the relationship between the SpP nanogels and the drugs under photostimulation. The method presented in this study introduces a new approach to drug loading and controlled release through the use of stimulus-responsive Sp-bearing pullulan.

CONCLUSIONS

An amphiphilic polymer (SpP) was synthesized via convenient attachment of light-responsive Sp molecules. The structure of starch was largely disrupted, and the A-type crystalline structure was transformed into a V-type one after the modification reaction. SpP can self-assemble into nanogels in aqueous solutions. The M_w and D_h of the nanogels significantly changed after irradiation under different wavelengths of light. Moreover, the nanogels exhibited a reversible light sensitivity when the wavelength is changed. The drug-loaded nanogels showed a light-controlled release behavior in drug-delivery systems. SpP is a novel stimulus-responsive amphiphilic nanogel that can be highly effective in drug delivery and tissue engineering. A model of quantity-controlled delivery was also presented. The results of this study can be used to develop customized systems that can deliver specific, rigidly controlled dosages to individual patients.

REFERENCES

1. Tan W.; Wang K.; Drake T. *J. Analyst* **2005**, *130*, 1003.

2. Peng, H. S.; Stolwijk, J. A.; Sun, L. N.; Wegener, J.; Wolfbeis, O. S. *Angew. Chem. Int. Ed.* **2010**, *49*, 4246.

3. Oishi, M.; Sumitani, S.; Nagasaki, Y. *Bioconjugate Chem.* **2007**, *18*, 1379.

4. Hasegawa, U.; Nomura, S. M.; Kaul, S. C.; Hirano, T.; Akiyoshi, K. *Biochem. Biophys. Res.* **2005**, *331*, 917.

5. Kobayashi, H.; Brechbiel, M. W. *Adv. Drug Delivery Rev.* **2005**, *57*, 2271.

6. Shen, J.; Song, Z.; Qian, X. *Appita J.* **2009**, *62*, 360.

7. Shen, J.; Song, Z.; Qian, X. *Bioresources* **2009**, *4*, 1190.

8. Van Tomme, S. R.; Hennink, W. E. *Expert Rev. Med. Devices* **2007**, *4*, 147.

9. Peppas, N. A.; Khare, A. R. *Adv. Drug Delivery Rev.* **1993**, *11*, 1.

10. Van Tomme, S. R.; Storm, G.; Hennink, W. E. *Int. J. Pharm.* **2008**, *355*, 1.

11. Qiao, Z. Y.; Zhang, R.; Du, F. S.; Liang, D. H.; Li, Z. C. *J. Controlled Release* **2011**, *152*, 57.

12. Steinhilber, D.; Sisson, A. L.; Mangoldt, D.; Welker, P.; Licha, K.; Haag, R. *Adv. Funct. Mater.* **2010**, *20*, 4133.

13. Peng, H. S.; Stolwijk, J. A.; Sun, L. N.; Wegener, J.; Wolfbeis, O. S. *Angew. Chem. Int. Ed.* **2010**, *49*, 4246.

14. Dai, S.; Ravi, P.; Tam, K. C. *Soft Matter* **2009**, *5*, 2513.

15. Katz, J. S.; Burdick, J. A. *Macromol. Biosci.* **2010**, *10*, 339.

16. Ercole, F.; Davis, T. P.; Evans, R. A. *Polym. Chem.* **2010**, *1*, 37.

17. Li, Y.; Jia, X. R.; Gao, M.; He, H.; Kuang, G. C.; Wei, Y. *J. Polym. Sci.* A1 **2010**, *48*, 551.

18. Lee, H. M.; Larson, D. R.; Lawrence, D. S. *ACS Chem. Biol.* **2009**, *4*, 409.

19. Uda, R. M.; Hiraishi, E.; Ohnishi, R.; Nakahara, Y.; Kimura, K. *Langmuir* **2010**, *26*, 5444.

20. Ferris, D. P.; Zhao, Y. L.; Khashab, N. M.; Khatib, H. A.; Stoddart, J. F.; Zink, J. I. *J. Am. Chem. Soc.* **2009**, *131*, 1686.

21. Coti, K. K.; Belowich, M. E.; Liong, M.; Ambrogio, M. W.; Lau, Y. A.; Khatib, H. A.; Zink, J. I.; Khashab, N. M.; Stoddart, J. F. *Nanoscale* **2009**, *1*, 16.

22. Agasti, S. S.; Chompoosor, A.; You, C.C.; Ghosh, P.; Kim, C.K.; Rotello, V. M. *J. Am. Chem. Soc.* **2009**, *131*, 5728.

23. Fu, G. D.; Xu, L. Q.; Yao, F. *ACS Appl. Mater. Interfaces* **2009**, *1*, 2424.

24. Li, M. H.; Keller, P. *Soft Matter* **2009**, *5*, 927.

25. Niu, Y. S.; Li, H. C. *Ind. Eng. Chem. Res.* **2012**, *51*, 12173.

26. Cao, S. L.; Song, D.; Deng, Y. L.; Ragauskas, A. *Ind. Eng. Chem. Res.* **2011**, *50*, 5628.

27. Das, K.; Dipa Ray, N. R. Bandyopadhyay, A. G.; Suparna Sengupta, S. S.; Mohanty, A.; Misra, M. *Ind. Eng. Chem. Res.* **2010**, *49*, 2176.

28. Na, K.; Bea, Y. H. *Pharm. Res.* **2003**, *19*, 681.

29. Chen, C. J.; Jin, Q.; Liu, G. Y.; Li, D. D.; Wang, J. L.; Ji, J. *Polymer* **2012**, *53*, 3695.

30. Zhao, Y. *Macromolecules* **2012**, *45*, 3647.

31. Garcia, A. A.; Cherian, S.; Park, J.; Gust, D.; Jahnke, F.; Rosario, R. *J. Phys. Chem. A* **2000**, *104*, 6103.

32. Rosario, R.; Gust, D.; Hayes, M.; Jahnke, F.; Springer, J.; Garcia, A. A. *Langmuir* **2002**, *18*, 8062.

33. Tan, J.; Li, Y.; Liu, R.; Kang, H.; Wang, D.; Ma, L.; Liu, W.; Wu, M.; Huang, Y. *Carbohydr. Polym.* **2010**, *81*, 213.

34. Namazi, H.; Dadkhah, A. *Carbohydr. Polym.* **2010**, *79*, 731.

35. Kapusniak, J.; Siemion, P. *J. Food Eng.* **2007**, *78*, 323.

36. Zou, W.; Liu, X.; Yu, L.; Qiao, D.; Chen, L.; Liu, H.; Zhang, N. *J. Polym. Environ.* **2013**, *21*, 359.

37. Liu H.; Yu L.; Simon G.; Dean K.; Chen L. *Carbohydr. Polym.* **2009**, *77*, 662.

38. Lu, X.; Luo, Z.; Yu, S.; Fu, X. *J. Agric. Food Chem.* **2012**, *60*, 9273.

39. Akiyama, E.; Morimoto, N.; Kujawa, P.; Ozawa, Y.; Winnik, F. M.; Akiyoshi K. *Biomacromolecules*, **2007**, *8*, 2366.

40. Kuroda, K.; Fujimoto, K.; Sunamoto, J.; Akiyoshi, K. *Langmuir* **2002**, *18*, 3780.

41. Hirakura, T.; Nomura,Y.; Aoyama,Y.; Akiyoshi, K. *Biomacromolecules* **2004**, *5*, 1804.

42. Li, Y.; Vries, R.; Kleijn, M.; Slaghek, T.; Timmermans, J.; Stuart, M. C.; Norde, W. *Biomacromolecules* **2010**, *11*, 1754.

43. Bysell, H.; Malmsten, M. *Langmuir* **2006**, *22*, 5476.

44. Lim Soo, P.; Luo, L; Maysinger, D.; Eisenberg, A. *Langmuir* **2002**, *18*, 9996.